Research Article Vol. 32, No. 26 / 16 Dec 2024 / Optics Express 46649
Optics EXPRESS

Dynamics of a high-energy fiber optical parametric chirped-pulse oscillator

Tristan Guezennec,[1,2] Saïd Idlahcen,[1] Laurent Provino,[2] Adil Haboucha,[2] Thomas Godin,[1,*] and Ammar Hideur[1]

[1]CORIA, UMR 6614 CNRS - INSA Rouen - Université de Rouen Normandie, Rouen, France
[2]Photonics Bretagne, Lannion, France
[*]thomas.godin@coria.fr

Abstract: We investigate the performances and noise characteristics of the recent concept of fiber optical parametric chirped-pulse oscillator (FOPCPO). Our FOPCPO is based on an in-house built functionalized nonlinear fiber for power handling and delivers broadly tunable pulses in the 820 nm (signal) and 1380 nm (idler) bands. Pulses can be dechirped to sub-500 fs duration with an energy up to 500 nJ. This system also exhibits an excellent RIN and we highlight that the cavity's feedback level is a key parameter that has a strong impact on the FOPCPO's dynamics. We eventually compare the oscillator and amplifier configurations for equivalent pump levels and show, through RIN and DFT analysis, that FOPCPOs prove superior in terms of noise properties, confirming their potential for nonlinear imaging and spectroscopy experiments where low noise levels are essential.

1. Introduction

Tunable high-energy ultrashort pulses generation from solid-state optical parametric chirped-pulse amplifiers and oscillators (OPCPA/OPCPO) is now routinely used in many scientific areas and drives a myriad of research and industrial applications [1]. Although they are not competitive regarding the available energy, fiber-based parametric sources relying on degenerate four-wave mixing (DFWM) stand out as they feature unique characteristics in terms of robustness and compactness. Specifically, they have proved relevant for various biophotonics applications such as multiphoton microscopy, stimulated Raman scattering (SRS), coherent anti-Stokes Raman scattering (CARS) imaging where their ability to deliver multi-wavelength, broadly-tunable and temporally synchronized ultrashort pulses at high repetition rates with relatively high energies enables fast acquisitions with low noises [2–5]. In order to upscale the energy of DFWM-based sources, the concept of fiber optical parametric chirped-pulse amplifier (FOPCPA) has been exploited in various configurations [6–8] and based on different types of fibers (PCF, DSF, photonic bandgap, birefringent) and allowed to reach the μJ level at 10 kHz repetition rate [9,10]. In particular, pumping in the normal dispersion regime enables the generation of signal/idler with a wide wavelength gap, up to several hundreds of nanometers [11–14], enabling the access to a wide range of molecular vibration levels, typically up to 4000 cm^{-1} when pumping in the 1 μm region. This feature makes these sources even more attractive for SRS applications [2]. Recently, this concept has been extended to oscillators, which have the advantage not to require a seed source, and where it has first been shown numerically that the chirp of the pump pulses acts as an extra parameter allowing to control the spectral bandwidth of the parametric pulses out of the cavity [15]. We then demonstrated experimentally the potential of such fiber optical parametric chirped oscillators (FOPCPO) pumped in the normal dispersion regime for the energy scaling of

#537887 https://doi.org/10.1364/OE.537887
Journal © 2024 Received 30 Jul 2024; revised 24 Sep 2024; accepted 28 Sep 2024; published 10 Dec 2024

Optics EXPRESS

broadly-tunable synchronized pulses [16] and highlighted that as in the FOPCPA schemes pulse energy scales with the pump chirp making the μJ barrier within the reach of FOPCPO. It is known from standard (non-chirped) systems that oscillators (FOPO) feature better noise properties than amplifiers (FOPA) [17], and this point is especially important regarding the biophotonics applications mentioned above. The purpose of this work is then twofold: (i) confirm the energy scaling possibilities of FOPCPO with sub-500 fs pulses using a functionalized fiber, which we previously demonstrated to handle multi-kW peak powers at high repetition rates [18], and (ii) investigate their dynamics, characterize their relative intensity noise (RIN) and identify the parameters driving their noise properties. This work is then structured as follows. We first present the normal-dispersion FOPCPO we developed around our custom-made nonlinear fiber and the diagnostic tools for characterizing the dynamics (RIN and dispersive Fourier transform). Then, after highlighting the performances (energy, compressed pulse duration, tunability) reached with this system, we investigate its noise properties and specifically study the impact of the cavity's feedback ratio on the dynamics. As this latter parameter adds complexity to FOPCPO relatively to FOPCPA, the last section of this work is thereby meant to quantitatively compare both systems and to spotlight the pros and cons of each scheme, depending on the targeted application.

2. Experimental set-Up

The experimental set-up of the FOPCPO studied in this work is depicted in Fig. 1(a). The pump laser is an in-house built Yb-doped fiber chirped-pulse amplified (FCPA) laser delivering 500 ps chirped pulses (200 fs transform limited) centered at 1036 nm at a repetition rate of 968 kHz and with an average power up to 10 W. As highlighted numerically in our previous study [16], where 140 ps pump pulses were used, pump pulses with a higher chirp could allow for the extraction of higher energies from the FOPCPO. The pump pulses are injected in a 8 cm long nonlinear fiber through a dichroic mirror and a 13.8 mm focal length aspheric lens. This air-silica microstructured fiber (SUP5-125, designed and drawn at Photonics Bretagne's facilities, hole diameter d = 1.4 μm, lattice pitch Λ = 3.2 μm) features a nonlinear coefficient of 15 $W^{-1}km^{-1}$, and a zero-dispersion wavelength (ZDW) of 1055 nm. In order to handle high pump powers, both ends of the fiber have been collapsed (see Fig. 1(c)) while preserving the output beam quality. Such a functionalized fiber has previously been shown to withstand several tens of kW peak power [18]. Signal and idler parametric pulses are generated in this fiber at widely-spaced wavelengths via DFWM according to the phase-matching diagram shown in Fig. 1(b). The FOPCPO cavity is then closed with a free-space adjustable-ratio circulator and a 200 m spool of 10 μm mode-field diameter polarization maintaining endlessely singlemode fiber (ESM10-PM, Photonics Bretagne). The circulator is based on a polarization beam splitter (PBS) combined with a quarter-wave plate allowing to direct the beam reflected by the ODL mirror into the ESM10-PM fiber. The PBS also acts as an output coupler.

The cavity length is set to be resonant on the signal pulse and adjusted using an optical delay line, which allows tuning the output spectrum of the FOPCPO through dispersive filtering [19]. The output pulses are filtered depending on the wavelength of interest (signal or idler) with edgepass filters (Thorlabs FELH1150/FESH0950), and eventually sent to diagnostics (optical / electrical spectrum analyzers, power-meter), a Treacy compressor (1200 grooves/mm), or a dispersive Fourier transform (DFT) setup for shot-to-shot spectral characterization [20]. The DFT setup consists of a 20 km long telecom grade dispersion compensating fiber spool, with a dispersion of approximately -2000 ps/nm at 1400 nm, a 30 GHz photodiode, and a 20 GHz real time oscilloscope, providing a 0.1 nm spectral resolution at 1400 nm. This setup allows tracking the idler pulses' dynamics and to check the FOPCPO stability. RIN measurements are carried out using an amplified photodiode (Thorlabs PDA015C, 44 dB built-in transimpedance amplifier), and a high resolution electrical spectrum analyzer (R&S FSV3030, 10 Hz-30 GHz).

Optics EXPRESS

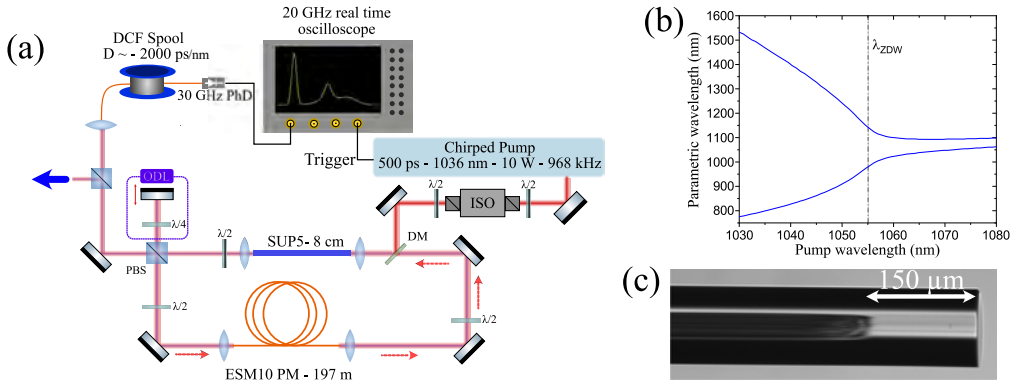

Fig. 1. (a) Experimental setup. ISO : Optical isolator. DM : Dichroic mirror. ODL : Optical delay line. PBS : Polarization beam splitter. DCF : Dispersion compensating fiber. PhD : Photodiode. (b) Phase-matching diagram of the SUP5-125 fiber. (c) Collapsed facet of the SUP5-125 fiber

3. Results on FOPCPO

Pumping the nonlinear fiber generates two parametric sidebands centered around 820 nm (signal) and 1400 nm (idler) and closing the cavity allows tuning the output pulses from 790 nm to 865 nm, and from 1310 nm to 1475 nm by adjusting the roundtrip delay through the optical delay line, as depicted in Fig. 2(a). This corresponds to a broad tunability of 75 nm for the signal and 165 nm for the idler. For a pump energy of 6 µJ (≈ 4.5 µJ injected in the nonlinear fiber, 500 ps duration), a maximum energy of 510 nJ (resp. 300 nJ) is obtained in the signal (resp. idler) out of the cavity, hence confirming the energy scaling on the pump chirp predicted numerically [16].

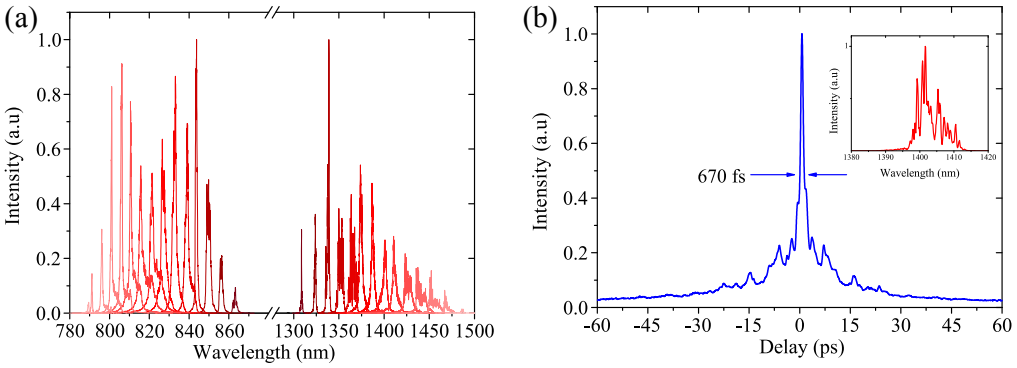

Fig. 2. FOPCPO's output characteristics. (a) Spectral tunability. Spectra have been normalized to the maximum intensity of their respective bands. (b) Autocorrelation trace of the compressed idler pulses. Inset: Corresponding spectrum.

The signal-resonant cavity design induces a strong chirp on the signal through the 200 m long feedback fiber, which should result in a narrowband idler as numerically predicted by Brinkmann et al. [15]. However, the strongly chirped pump pulses used here lie outside the studied scenarios. In our case, since the chirp of the pump pulses (~36.1 ps^2 from the FCPA stretcher) is higher than the one of the signal pulses (~6.4 ps^2 from the feedback fiber), the latter are only slightly chirped with a narrow spectrum (from 0.5 nm to 2 nm) and the idler pulses are strongly chirped with a broad spectrum (from 2 nm to 10 nm). The idler pulses have been dechirped from 150 ps to

Optics EXPRESS

448 fs (estimated from the autocorrelation trace depicted in Fig. 2(b) assuming Gaussian-shaped pulses), which is close to the theoretical limit as the corresponding spectrum (inset in Fig. 2(b)) provides a 440 fs Fourier-limited duration.

From our experiments, the cavity feedback level seemed to be a key parameter driving the system dynamics and its noise properties. In order to quantitatively investigate its impact, RIN measurements have been performed with two different feedback powers, estimated from non-perturbative measurements via Fresnel's reflections on a glass plate at the output of the feedback fiber. In the following, the low feedback level corresponds to a re-injected power of 70 μW while the high level corresponds to 600 μW. RINs in both cases are compared in Fig. 3, where it can clearly be seen that the cavity with a lower feedback ratio (blue line) produces idler pulses with a lower noise, around 10 dBc/Hz below the high feedback cavity (black line). In addition, even lower feedback levels have been tested (down to 6 μW) but lead to a deterioration of the RIN and the 70 μW feedback level has been found to be optimal. This value has been found empirically, by adjusting the feedback ratio while monitoring the output pulse energy along with the signal bandwidth, as the latter broadens when the regime becomes unstable as discussed in Ref. [21]. It can also be seen that the noise from the pump laser is transferred to the idler pulses, particularly the relaxation peak at 22 kHz. The overall RIN sets below -120 dBc/Hz, and eventually reach -150 dBc/Hz at $f_{rep}/2$, hence qualifying the FOPCPO for nonlinear spectroscopy applications, as some commercial CARS systems certify sub -145 dBc/Hz RIN levels. In the end, the RIN could be further lowered by enhancing the pump stability, as already suggested in a previous work [3], and as it can be required for specific SRS applications [22]. These measurements then confirm that a specific attention has to be paid to the cavity feedback ratio when designing a FOPCPO targeting applications where low noise levels are required.

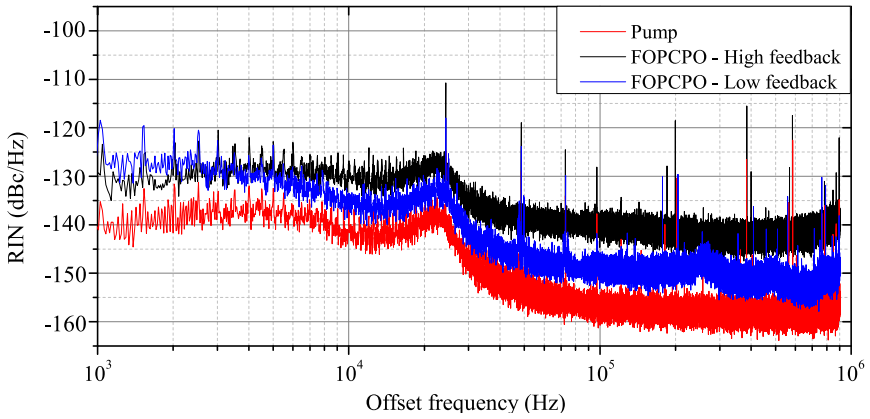

Fig. 3. Relative intensity noise (RIN) measurements of the idler pulses for a low, optimal cavity feedback level (blue line) and for a higher level (black line). The pump RIN is plotted as a red line as a reference.

In addition, DFT measurements were performed on the idler pulses to confirm the stable operation of the FOPCPO. We then recorded 800 consecutive shot-to-shot spectra (i.e. roundtrips in the cavity) of the FOPCPO, as shown in Fig. 4. From the time-stretched traces, we inferred a 4% deviation from the mean detected peak power and observed that the spectra are consistent from one pulse to another, attesting again the system's stability. The same tools - RIN and DFT - will be used in the following to compare the noise properties of FOPCPO and FOPCPA.

Optics EXPRESS

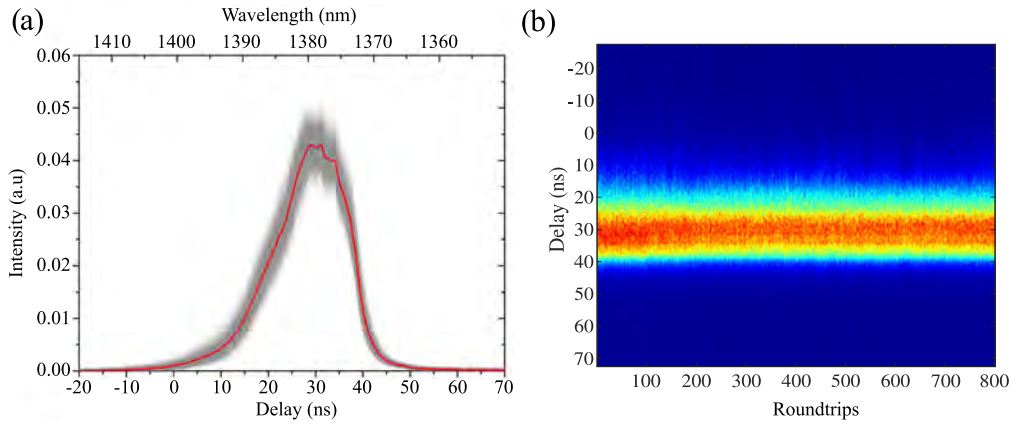

Fig. 4. (a) Measurement of 800 consecutive shot-to-shot idler spectra (gray) through dispersive Fourier transform (DFT), in a stable regime. Their mean is shown as a red line. (b) Consecutive spectra stacked horizontally for visualization.

4. Comparison with a FOPCPA

In order to evaluate and compare the overall performances of the FOPCPO, we implemented a FOPCPA by injecting a continuous-wave 810 nm seed signal (single-mode laser diode from Aerodiode) in the nonlinear fiber without any feedback loop while keeping the other parameters identical to the previous experiment. The FOPCPA exhibits similar performances as the FOPCPO (at the same wavelength tuning, i.e. 1436 nm for the idler), namely pulses energies up to 300 nJ, and a dechirped duration of 400 fs, as depicted in Fig. 5. However, it is worth noting that the autocorrelation trace of the dechirped FOPCPA idler pulses exhibits a larger pedestal than the pulses from the FOPCPO (Fig. 2(b)), which can be attributed to an excess of nonlinear phase, arising for example from a slightly too long nonlinear fiber, or transferred directly from the pump pulses. The RIN was then measured with two seeding power levels: 3 mW and 40 mW. As reported in a previous work on standard FOPOs [17], and as depicted in Fig. 6, the FOPCPA exhibits higher RINs for the same pump energy (3 μJ here), with a plateau above -130 dBc/Hz for the sub-seeded FOPCPA. This striking difference between the FOPCPO and the FOPCPA noise performances could be attributed to either an additional noise source, namely the seeding laser diode, or the absence of a feedback loop that stabilizes the regime.

To investigate the impact of seeding level on the noise characteristics, we performed another set of DFT measurement on the FOPCPA. By seeding the FOPCPA with only 0.3 mW, it can be seen in Fig. 7(a) that the regime is highly unstable, leading to a noisy output, with a 35% deviation from the mean detected peak power, hindering the use of such a source in any nonlinear imaging setup. By increasing the seeding power up to 3 mW, it can be shown that the pulses are getting more stable, as depicted in Fig. 7(b), showing again a clear relation between the seeding power and the parametric pulses noise characteristics. In addition, to quantify the noise from the DFT measurements, we used the signal-to-noise ratio (SNR) proposed by Guilberteau et al. [23]. As a reference, we calculated a SNR of 16 from the stable DFT measurement of the FOPCPO output depicted in Fig. 4. From the measurements depicted in Fig. 7, we then calculated a SNR of 3 for the unstable case and 11 for the stable case, confirming again the relevance of FOPCPO when low noise levels are needed.

Optics EXPRESS

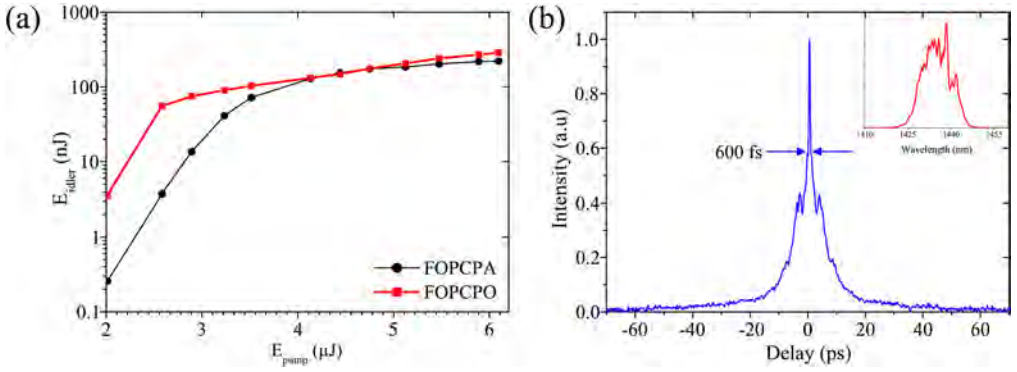

Fig. 5. Performances of the FOPCPA at 40 mW seed power. (a) Idler energy versus pump energy (black line) and comparison with the FOPCPO configuration (red line). b) Autocorrelation trace of the compressed idler pulses. The corresponding spectrum is shown in the inset.

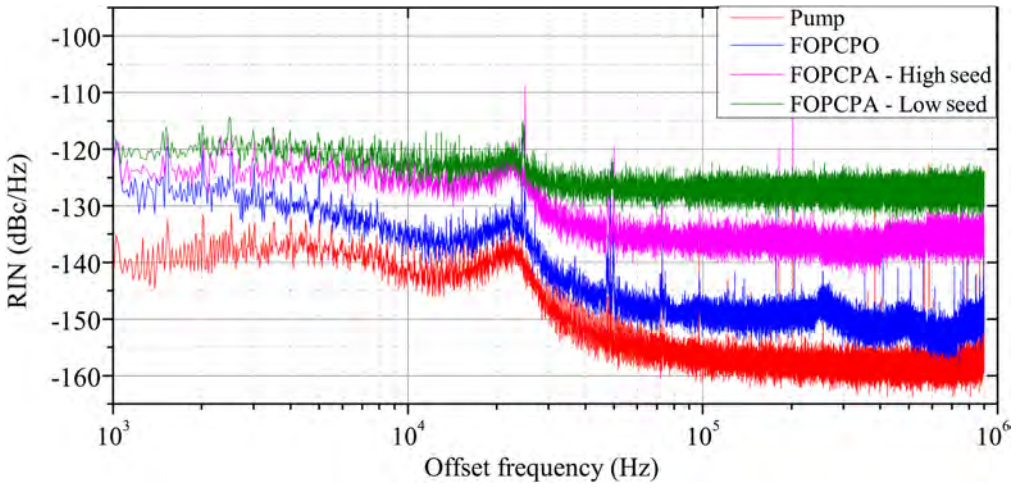

Fig. 6. Comparison of the RIN of the FOPCPO and pump (previous section) with the RIN of the FOPCPA (idler) for high (pink line) and low (green line) seeding levels at 810 nm.

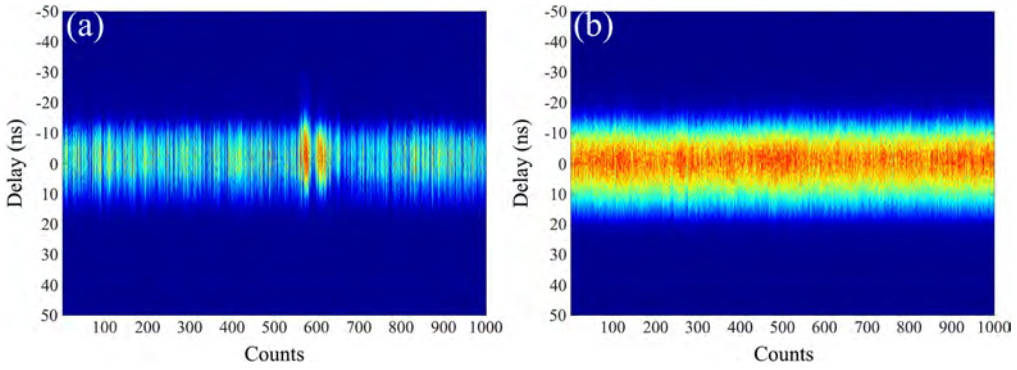

Fig. 7. Measurement of 1000 consecutive shot-to-shot idler spectra through DFT in the FOPCPA configuration, for two different seeding powers: (a) 0.3 mW and (b) 3 mW.

Optics EXPRESS

5. Conclusion

We demonstrated in this work the potential of normal-dispersion FOPCPOs for the generation of high-energy, low noise and broadly-tunable ultra-short pulses at high repetition rates. When operated with an optimal cavity feedback level, the FOPCPO exhibits a remarkably low RIN, an energy up to 500 nJ, with pulses that can be dechirped down to less than 500 fs. We highlighted that the feedback level is a key parameter when designing such a source for applications where good noise properties are mandatory. In addition, we evidenced that FOPCPA schemes exhibit higher RIN levels than FOPCPOs for a similar pumping level, but remains simpler to implement and thereby could be used when very low noise levels are not required. We also showed that the pump RIN is transferred to the parametric pulses via the four wave mixing process and, as a consequence, enhancing the performances of the pump source should lower the RIN of the FOPCPO. We eventually demonstrated that using highly chirped pump pulses, along with a functionalized nonlinear fiber in order to withstand high peak powers, enables the generation of high energy pulses from a fiber optical parametric oscillator.

Funding. Association Nationale de la Recherche et de la Technologie; Région Bretagne; Région Normandie; Agence Nationale de la Recherche; Institut Carnot Energie et Systèmes de Propulsion.

Disclosures. The authors declare no conflicts of interests.

Data availability. The data generated in this work are available upon reasonable request.

References

1. A. Dubietis and A. Matijošius, "Table-top optical parametric chirped pulse amplifiers: past and present," Opto-Electron. Adv. **6**(3), 220046 (2023).
2. T. Gottschall, T. Meyer, and M. Baumgartl, "Fiber-based light sources for biomedical applications of coherent anti-stokes raman scattering microscopy," Laser Photonics Reviews **9**(5), 435–451 (2015).
3. M. Brinkmann, S. Janfrüchte, and T. Hellwig, "Electronically and rapidly tunable fiber-integrable optical parametric oscillator for nonlinear microscopy," Opt. Lett. **41**(10), 2193–2196 (2016).
4. C. Kong, C. Pilger, and H. Hachmeister, "High-contrast, fast chemical imaging by coherent raman scattering using a self-synchronized two-colour fibre laser," Light: Sci. Appl. **9**(1), 25 (2020).
5. M. Brinkmann, A. Fast, and T. Hellwig, "Portable all-fiber dual-output widely tunable light source for coherent raman imaging," Biomed. Opt. Express **10**(9), 4437–4449 (2019).
6. Y. Zhou, Q. Li, and K. K. Cheung, "All-fiber-based ultrashort pulse generation and chirped pulse amplification through parametric processes," IEEE Photonics Technol. Lett. **22**(17), 1330–1332 (2010).
7. V. Cristofori, Z. Lali-Dastjerdi, and L. S. Rishøj, "Dynamic characterization and amplification of sub-picosecond pulses in fiber optical parametric chirped pulse amplifiers," Opt. Express **21**(22), 26044–26051 (2013).
8. Y. Qin, Y.-H. Ou, and B. Cromey, "Watt-level all-fiber optical parametric chirped-pulse amplifier working at 1300 nm," Opt. Lett. **44**(14), 3422–3425 (2019).
9. P. Morin, J. Dubertrand, and P. B. d'Augeres, "μj-level raman-assisted fiber optical parametric chirped-pulse amplification," Opt. Lett. **43**(19), 4683–4686 (2018).
10. L. Lafargue, F. Scol, and O. Vanvincq, "All-polarization-maintaining and high-energy fiber optical parametric chirped-pulse amplification system using a solid core photonic hybrid fiber," Opt. Lett. **47**(17), 4347–4350 (2022).
11. W. Fu and F. W. Wise, "Normal-dispersion fiber optical parametric chirped-pulse amplification," Opt. Lett. **43**(21), 5331–5334 (2018).
12. Y. Qin, O. Batjargal, B. Cromey, *et al.*, "All-fiber high-power 1700 nm femtosecond laser based on optical parametric chirped-pulse amplification," Opt. Express **28**(2), 2317–2325 (2020).
13. W. Fu, R. Herda, and F. W. Wise, "Design guidelines for normal-dispersion fiber optical parametric chirped-pulse amplifiers," J. Opt. Soc. Am. B **37**(6), 1790–1805 (2020).
14. M. L. Buttolph, P. Sidorenko, C. B. Schaffer, *et al.*, "Femtosecond optical parametric chirped-pulse amplification in birefringent step-index fiber," Opt. Lett. **47**(3), 545–548 (2022).
15. M. Brinkmann, T. Hellwig, and C. Fallnich, "Optical parametric chirped pulse oscillation," Opt. Express **25**(11), 12884–12895 (2017).
16. R. Becheker, M. Touil, and S. Idlahcen, "High-energy normal-dispersion fiber optical parametric chirped-pulse oscillator," Opt. Lett. **45**(23), 6398–6401 (2020).
17. E. S. Lamb, S. Lefrancois, and M. Ji, "Fiber optical parametric oscillator for coherent anti-stokes raman scattering microscopy," Opt. Lett. **38**(20), 4154–4157 (2013).
18. T. Guezennec, S. Idlahcen, and A. Cervera, "μj-level normal-dispersion fiber optical chirped-pulse parametric oscillator," J. Eur. Opt. Society-Rapid Publ. **20**(1), 7 (2024).
19. Y. Zhou, K. K. Y. Cheung, and S. Yang, "Widely tunable picosecond optical parametric oscillator using highly nonlinear fiber," Opt. Lett. **34**(7), 989–991 (2009).

Optics EXPRESS

20. T. Godin, L. Sader, A. Khodadad Kashi, *et al.*, "Recent advances on time-stretch dispersive fourier transform and its applications," Adv. Phys.: X **7**, 2067487 (2022).
21. W. Q. Zhang, J. E. Sharping, and R. T. White, "Design and optimization of fiber optical parametric oscillators for femtosecond pulse generation," Opt. Express **18**(16), 17294–17305 (2010).
22. X. Audier, S. Heuke, and P. Volz, "Noise in stimulated Raman scattering measurement: From basics to practice," APL Photonics **5**(1), 011101 (2020).
23. T. Guilberteau, C. Fourcade-Dutin, and F. Fauquet, "Noise analysis in a seeded four-wave mixing process generated in a photonic crystal fiber pumped by a chirped pulse," Opt. Lett. **48**(11), 2905–2908 (2023).